Journal of Molecular Modeling (2020) 26:51
https://doi.org/10.1007/s00894-020-4314-y

ORIGINAL PAPER

# Experimental and theoretical studies of electrochemical oxidation of nicotinamide adenine dinucleotide at the modified SWCNT and graphene oxide

İzzet Koçak[1] · Hakan Alıcı[2]

Received: 9 October 2019 / Accepted: 28 January 2020


**Abstract**
In recent years, nicotinamide adenine dinucleotide (NADH) and its oxidized form ($NAD^+$) have withdrawn a substantial attention since they possess a significant place in both biosensor and biofuel cell studies. However, the transformation of NADH to $NAD^+$ brings about the surface passivation and fouling at the most of corresponding conductive materials; consequently, significant decrease takes place in the current. In order to overcome these drawbacks, we have performed the surface functionalization of single-walled carbon nanotube (SWCNT) and graphene oxide (GO) immobilized onto glassy carbon surface with dihydroxybenzene (di-HB) using solid-phase synthesis methodology. The di-HB-modified SWCNT and GO were found to exhibit great catalytic activity as they reduce required overpotential of electrochemical oxidation of NADH and lead to enhancement in the peak current, compared with unmodified carbon electrodes. Molecular docking simulation technique was also carried out to enlighten attained experimental findings in detail, and we have found that increase in the binding affinity of $NAD^+$ to functionalized carbon surfaces with di-HB is related to formation of hydrogen bonding interactions Furthermore, our experimental and theoretical outputs were also found to be quite consistent in terms of reactivity of modified surfaces to NADH oxidation.

**Keywords** $NAD^+$ · SWCNT · Graphene · Docking

## Introduction

Nicotinamide adenine dinucleotide (NADH) is generally regarded as one of the most significant biological compounds due to its vital role in biological electron transfer mechanism, and it acts as cofactor for the numerous amounts of dehydrogenase [1, 2]. The transformation of NADH to $NAD^+$ is literally an $H^-$ transfer through obtaining 2 electrons and 1 proton. However, it is still not clear that if the electrochemical oxidation of NADH to $NAD^+$ proceeds sequentially or follows a one-step mechanism [3]. The development of electrodes that are able to convert NADH to $NAD^+$ has also aroused considerable interest among the scientist on account of their plausible application in the area of biosensors. The transformation of NADH to $NAD^+$ at the unmodified electrodes demonstrates irreversible electrochemical process, and one of the well-known specialties of this reaction is the large activation barrier, as a result of which the regarding anodic irreversible peak arises at more positive potential [4–6]. It is also noteworthy that NADH and its oxidized form, $NAD^+$, can quite constantly be adsorbed, which provokes the fouling at the electrode surface and consequently a diminishment in the passing peak current. If this issue is not fixed in the biosensors systems, it causes an interference owing to the generation of side moieties during electrochemical oxidation process, lack of sensitivity, reproducibility, and stability [7, 8]. In order to get rid of above-mentioned complications, a great deal of effort has been devoted to discover applicable mediators, capable of making the

**Electronic supplementary material** The online version of this article (https://doi.org/10.1007/s00894-020-4314-y) contains supplementary material, which is available to authorized users.

✉ İzzet Koçak
kocakizzet@gmail.com

[1] Faculty of Pharmacy, Zonguldak Bülent Ecevit University, Zonguldak, Turkey

[2] Department of Physics, Faculty of Science and Art, Zonguldak Bülent Ecevit University, Zonguldak, Turkey

Published online: 07 February 2020

electron transfer between NADH and the substrate much faster, such as quinone derivatives [9], catechol [10], ferrocene [11], ruthenium, or zinc complexes [12]. In the case of the architecture of suitable electrode, a relevant mediator should be able to reduce overvoltage of the reaction in order to abstain from interferences that stem from species formed in the course of electrochemical oxidation of NADH. Ghanem et al. reported that the coupling of chemical compound bearing hydroxyl groups possesses the catalytic influence on the NADH oxidation since there is an enhancement in the peak current and a shift toward less positive potential with respect to plain glassy carbon (GC) electrodes [9]. Pumera et al. also illustrated that edge and basal sites of the graphene sheet exhibit significantly different reactivity toward NADH oxidation using a molecular dynamic simulation [8]. It was also stated that if $NAD^+$ is placed near the basal and H-terminated edge sites of graphene sheet that also includes carboxyl and hydroxyl groups, there is a strong interaction between $NAD^+$ and the carboxyl and hydroxyl groups at the edge site; however, no remarkable energy is attained in the case of $NAD^+$ oriented near the basal site of graphene or edge sites of graphene only terminated with hydrogen. Since the wall and tube ends of the SWCNT could be regarded as basal and edge sites, respectively, the same research group considered that it would also be quite interesting to investigate how different regions of SWCNT act to NADH oxidation by using the identical Car–Parrinello molecular dynamics simulation technique [13]. They eventually achieved similar theoretical findings to their previous study in terms of reactivity of wall and tube ends to NADH oxidation.

We have reported here the modification of SWCNT and GO electrodes with dihydroxybenzene (di-HB) and NADH oxidation at the regarding di-HB-modified carbon electrodes. The di-HB-modified graphene and SWCNT electrodes were shown to possess noticeable influence on the electrochemical NADH oxidation as significant increase in the peak current and reduction in the overpotential were observed confronted with unmodified carbon surfaces. Hence, the verification of the reactivity of di-HB-modified SWCNT and graphene oxide with respect to both plain carbon electrodes by using a molecular docking simulation technique, AutoDock 4.2, would be a novel and interesting study. In terms of the tendency of SWCNT and graphene oxide to participate interaction with $NAD^+$, our experimental and theoretical results were shown to be in quite good agreement.

## Materials and methods

### Electrochemical measurements and modification of SWCNT and graphene oxide

All electrochemical measurements were carried out with SP-50 model Biologic Science Instruments potentiostat/galvanostat and controlled using EC-Lab software (GPES), a conventional three-electrode system that is composed of working electrode and platinum wire as the counter electrode, and a saturated calomel electrode (SCE) was used as the reference electrode. Electrografting of mono-tert-butyloxycarbonyl protecting group (Boc)–protected ethylenediamine linker (Boc-EDA) to carbon nanotube and graphene electrodes was performed by electrochemical oxidation from the corresponding solutions consisting of 10 mM Boc-EDA and 0.1 M tetrabutylammonium tetrafluoroborate (TBATFB) in acetonitrile (ACN) [14–16]. The modification of electrodes was performed by cycling the electrode potential from 0.7 to 2.2 V versus SCE. After successful electrochemical attachment of Boc-EDA linker, all electrodes were placed in 4 M HCl in dioxane at room temperature for 1 h to remove Boc protecting group [17]. The electrode was then rinsed by dimethylformamide (DMF), deionized water, and absolute ethanol. Coupling of acetyl chloride at the modified carbon electrode was also carried out as follows. (3,4-dimethoxyphenyl)-acetyl chloride (1 mmol) was dissolved in dichloromethane-pyridine 1:1. Modified electrodes were allowed to react with this solution for 16 h at room temperature. The conversion of the methoxy to hydroxyl groups was eventually performed with 1 M of $BBr_3$ for 1 h. The attachment of SWCNTs to GC surface was carried out by placing 5 mg of SWCNTs in 1 mL of ethanol followed by ultrasonic agitation. The resulting suspension of SWCNTs was then pipetted on GC. The solvent was allowed to be evaporated at room temperature. The synthesis of graphene oxide was also the same as given literature [18, 19]. The preparation of SWCNT and graphene oxide electrode was carried out as follows: 5 mg of SWCNTs or GO was sonicated in 1 mL of DMF followed. The obtained 10 μL of suspension either SWCNT or GO was then deposited on the mirror like polished glassy carbon electrode surface. The resulting electrodes were allowed to be kept at room temperature to evaporate the solvent.

### Molecular docking simulation studies

#### Structural preparation

The 3D structure of $NAD^+$ molecule was drawn and protonated by using Avogadro v1.2.0 [20], and then, its geometries were optimized with the MMFF94s force field using energy minimization protocols of this software. On the other hand, for docking simulations, we have handled four target structures, namely, SWCNT, SWCNT/di-HB, graphene, and graphene/di-HB. These target structures were sketched by using PyMOL [21]. Before the docking simulations, Kollman charges and non-polar hydrogens were added to target structures whereas Gasteiger charges, and nonpolar hydrogens

were added to each atom of $NAD^+$ by using AutoDock Tools [22].

### Docking

The docking simulations were performed by AutoDock 4.2. Each molecular docking process consists of long 1000 simulation runs with the Lamarckian genetic algorithm (LGA) method [22, 23], which is known to be a reliable method for AutoDock. These LGA runs were applied by creating an initial population of 150 individuals and a maximum 2,500,000 energy evaluations. In our docking simulations, the $NAD^+$ and di-HB molecules were selected as flexible while the SWCNT and graphene structures were selected as rigid. On the other hand, the grid maps were calculated using AutoGrid. In here, the grid map with a grid-point spacing of 0.375 Å was set as $90 \times 90 \times 100$ Å for SWCNT and SWCNT + di-HB points and as $90 \times 120 \times 50$ Å for graphene and graphene + di-HB points. In the calculations, the other parameters were set as default: external grid energy 1000.0 number of top individuals to survive to next generation 1; rate of gene mutation 0.02; rate of crossover 0.8; alpha parameter of Cauchy distribution 0.0; beta parameter Cauchy distribution 1.0; iterations of Solis and Wets local search 300; consecutive successes before changing rho 4; consecutive failures before changing rho 4; size of local search space to sample 1.0; lower bound on rho 0.001; and probability of performing local search on individual 0.06.

After the docking operation is completed, the binding modes of $NAD^+$ were clustered using a root mean square (RMS) tolerance of 2 Å, and then, these clustered conformations were ranked on the basis of free energy of binding. Finally, three best binding poses for each docking simulation systems were chosen and displayed. Visual analysis of the interaction of docked systems was performed using the Biovia DS Visualizer software [24].

## Results and discussion

The covalent attachment of ethylenediamine bearing Boc protecting group to SWCNT or GO immobilized onto glassy carbon electrode was achieved by electrochemical oxidation of corresponding linker in ACN, as given in detail in the "Materials and methods" section and research papers [16, 17]. The obtained voltammograms for each carbon electrode was found to be consistent with our previous paper, and hence, CVs of electrochemical grafting of Boc-EDA at SWCT and GO were not presented in this work. The coupling of di-HB is also achieved by following the methodology detailed in the regarding literature [25]. As illustrated in Scheme 1, subsequent to the coupling of (3,4-dimethoxyphenyl) acetyl chloride to SWCNT and graphene oxide surfaces, deprotection of the methoxy group is achieved with $BBr_3$ (1 M in dichloromethane). As seen, well-defined voltammograms (red solid lines) are obtained for all carbon electrodes by cyclic voltammetry technique in aqueous solution.

Figure 1 shows the cyclic voltammograms obtained for the single-walled carbon nanotube (Fig. 1a) and graphene oxide (Fig. 1b) electrodes in buffer (pH = 7) solution in the absence and presence of NADH at the scan rate of 50 $mVs^{-1}$. Black and red solid lines represent voltammograms recorded for unmodified and di-HB-modified SWCNT and GO electrodes in NADH-free solution. Blue and green solid lines also correspond to cyclic voltammograms obtained for plain and di-HB-modified SWCNT and GO electrodes in the presence of NADH. As clearly seen, cyclic voltammograms for both functionalized carbon electrodes type demonstrate well-defined reversible peaks with potential $E_{mp}$ of − 0.143 V and 0.182 mV vs SCE for di-HB-modified SWCNT and GO, respectively. This such difference in the redox potential of di-HB-modified SWCNT and GO in the absence of NADH could be linked to the fact that the proportion of edge sites at the SWCNT is more abundant compared with GO. Because it is well established that the edge sites increases across the carbon surfaces, tendency to participate in electrochemical

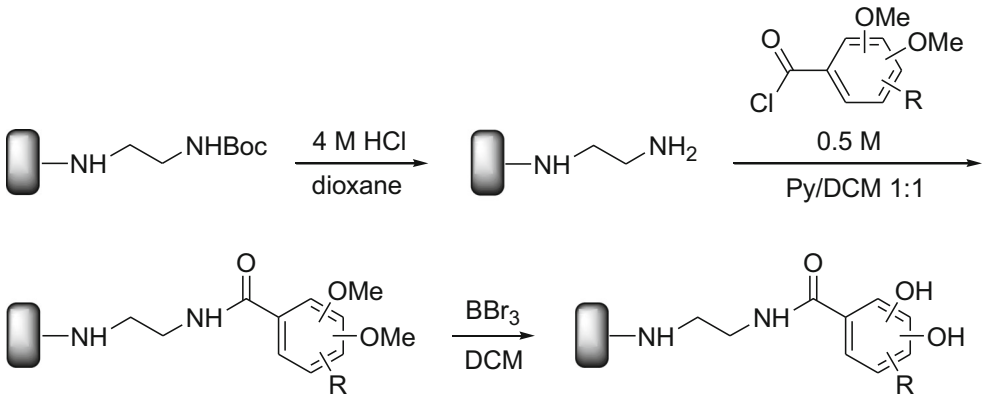


**Scheme 1** General systematic representation of coupling of di-HB derivative to functionalized SWCNT and GO through electrochemical oxidation of Boc-protected ethylenediamine.

process become more facile, which leads to shift in the peak potential toward less positive potential [4]. It should also be stated that obtained voltammograms for both di-HB-modified carbon electrodes (Fig. 1a, b (red solid lines)) seem to be rather stable due to the fact that voltammograms obtained for di-HB-modified SWCNT and GO electrodes during the first cycle exhibit 5% and 8% larger reduction peak currents for SWCNT and GO, respectively. Decrease in the peak current presumably probably stems from the detachment of non-covalently attached di-HB molecules.

The covalent attachment of dihydroxybenzene derivative to conductive surfaces was thought to have electrocatalytic activity for NADH oxidation, which is commonly considered a very significant coenzyme in the living organism. It is therefore attention-grabbing to note that the cyclic voltammograms recorded for both electrodes in buffer solution containing 1 mM of NADH gave rise to enhancement in the peak current and positive shift in the oxidation peak potential. As can be seen from Fig. 1a, b, since NADH oxidation takes place in the bare SWCNT and GO around 270 mV and 300 mV (blue solid lines), the overpotential of NADH oxidation is significantly reduced by both the di-HB-modified carbon electrodes with the anodic peak potential of 200 mV and 240 mV (green solid lines) for SWCNT and GO, respectively. It is also quite interesting to note that decrease in the overpotential for NADH oxidation at the di-HB-modified SWCNT is larger by approximately 10 mV relative to modified GO, which could be attributed to the surface properties and morphology of the different carbon electrodes, which refers to the fact that edge site proportion at the SWCNT is more abundant than GO. It is well-known that edge sites are quite abundant in terms of oxygenated functional groups, such as phenols, quinones, and carboxylic acid, and unsatisfied valences. It is thus assumed that as the edge proportion increases at the surface, the tendency of reacting of any chemical or biological compound with surface bearing oxygenated functional group is more likely. Therefore, when we introduced di-HB (possesses hydroxyl group) to graphene oxide and SWCNT, it is intrinsically expected that reaction between NADH and modified SWCNT takes place more facile, and as consequence of this output, the overpotential of NADH oxidation appears at the less positive potential for di-HB-modified SWCNT and GO in comparison with bare carbon electrodes. On the other hand, there are some peaks appearing on the voltammograms of NADH oxidation recorded for modified SWCNT and GO. In order to identify the origin of these peaks, CV measurements were run in the case of the non-modified electrodes. As clearly seen in Fig. 1 a and b sketched for non-modified electrodes in the absence (black solid lines) and presence of NADH (blue solid lines), especially, there are some cathodic peaks appearing on the voltammograms recorded for the bare SWCNT and GO. When the CV obtained for plain and di-HB-modified carbon electrodes in the absence and presence of NADH were taken into account together, those cathodic peaks might be ascribed to electrochemical reduction of the oxygenated functionalities that could be generated during electrochemical grafting of Boc-protected ethylenediamine and solid phase synthesis methodology to couple di-HB derivative or electrochemical reduction of trace amount of oxygen present in the buffer solution. Because there are absolutely no peaks available on the voltammograms recorded for non-modified electrodes in the NADH-free buffer solution.

Furthermore, difference in the formal potential of NADH for both di-HB-modified SWCNT and GO could be attributed to the onset potential of NADH oxidation that is necessary to initiate electrochemical process. Baez et al. investigated the influence of the starting potential on the electrochemical oxidation of NADH at the glassy carbon electrode modified with graphene oxide (GO) and SWCNT [26]. It was shown that as the electrochemical oxidation of the NADH is initiated at the more negative potential, formal potential of the NADH oxidation shifts toward a more negative potential. This such interesting behavior could be associated with occurrence of in situ electrochemical reduction of oxygenated functionalities

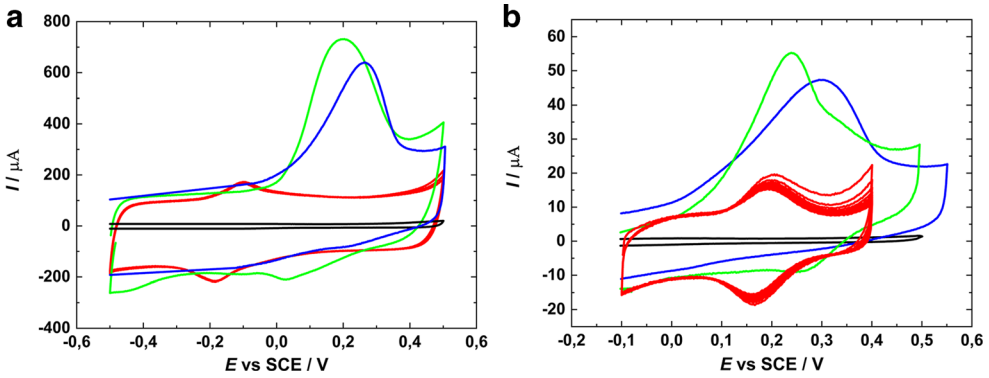


**Fig. 1** Cyclic voltammograms recorded at the scan rate of 50 mV $s^{-1}$ for plain and di-HB-modified SWCNT (**a**) and GO (**b**) in the absence and presence of 1 mM of NADH in 0.1 M phosphate buffer, pH 7. Black and red solid lines represent CVs in NADH-free buffer solution for plain and di-HB-modified electrodes, respectively. Blue and green solid lines correspond to voltammograms recorded for plain and di-HB-modified electrodes in the presence of NADH, respectively

**Table 1** Binding energy values, interaction types between $NAD^+$ and target structures, number of interaction for each, and interacting atoms of $NAD^+$

| Target | Pose | Binding energy (kcal/mol) | Interactions |
|---|---|---|---|
| SWCNT | 1 | − 18.14 | 7[pp] (E) + 6[pp] (D) + 7[pp] (A) + 2[pc] (10) + 2[pa] (35) + 2[pa] (31) + 1[pL] (36) + 1[pL] (26) + 1[pS] (59) |
| | 2 | − 18.01 | 8[pp] (E) + 5[pp] (D) + 7[pp] (A) + 3[pc] (10) + 4[pa] (35) + 2[pa] (31) + 1[pL] (36) + 1[pL] (26) + 1[pL] (32) + 1[pS] (60) + 1[pS] (47) |
| | 3 | − 17.92 | 7[pp] (E) + 8[pp] (D) + 7[pp] (A) + 3[pc] (10) + 1[pL] (36) + 1[pS] (47) |
| SWCNT/di-HB | 1 | − 23.52 | 6[pp] (E) + 7[pp] (D) + 8[pp] (A) + 2[pc] (10) + 2[pa] (35)+ 1[pL] (34)+ 1[pL] (20) + 1[pL] (3) + [pD] (64) |
| | 2 | − 23.33 | 8[pp] (E) + 8[pp] (D) + 2[pp] (A) +2[pc] (10) + 1[pa] (31) + 1[pL] (22) + 1[pL] (34) + 1[pS] (24) |
| | 3 | − 23.26 | 8[pp] (E) + 8[pp] (D) + 5[pp] (A) + 3[pc] (10) + 1[pL] (34) + 1[pL] (20) + 1[pL] (44) + 1[pS] (24) |
| Graphene | 1 | − 12.39 | 10[pp] (E) + 11[pp] (D) + 10[pp] (A) + 4[pc] (10) + 2[pa] (31) + 1[pL] (34) + 1[pL] (20) + 1[pS] (23) |
| | 2 | − 12.34 | 10[pp] (E) + 10[pp] (D) + 12[pp] (A) + 5[pc] (10) + 3[pa] (31) + 1[pL] (34) + 1[pL] (22) |
| | 3 | − 11.30 | 9[pp] (E) + 9[pp] (D) + 11[pp] (A) + 4[pc] (10) + 1[pL] (36) + 1[pL] (20) + 1[pL] (3) + 1[pL] (30) + 1[pS] (65) |
| Graphene/di-HB | 1 | − 15.71 | 11[pp] (E) + 12[pp] (D) + 12[pp] (A) + 5[pc] (10) + 3[pa] (35) + 1[pL] (3) + 1[pL] (20) + 1[pL] (30) + [pD] (63)+ 1[pS] (58) |
| | 2 | − 15.69 | 12[pp] (E) + 12[pp] (D) + 10[pp] (A) + 7[pc] (10) + 4[pa] (35) + 1[pL] (3) + 1[pL] (34) + [pD] (46) + 1[pS] (59) |
| | 3 | − 15.66 | 12[pp] (E) + 11[pp] (D) + 12[pp] (A) + 5[pc] (10) + 5[pa] (35) + 1[pL] (20) + 1[pS] (65) |

[pp] pi-pi stacked, [pa] pi-anion interaction, [pc] pi-cation interaction, [pL] pi-lone pair interaction, [pS] pi-sigma interaction, [pD] pi-donor interaction. Indexes within the parentheses represent atom or atom groups

that exists at the GO surface in case electrochemical process is adequately started at the more negative potential. Therefore, if NADH oxidation is commenced at the more negative potential, the oxidative species present at the GO structure is electrochemically reduced, and catalytic activity to NADH oxidation becomes more favorable. The effect of the onset potential was also studied by the same research group for SWCNT electrode for the electrochemical oxidation of NADH, and it was clearly stated in the literature that there was no influence of starting potential of electrochemical process on the formal potential of NADH oxidation.

The sensitivity of the di-HB-modified SWCNT and GO was investigated by altering the concentration of NADH, ranging from 1 to 30 μ mol $L^{-1}$, through using differential pulse voltammetry (DPV). Figs. S1 and S2 show the relationship between change in the peak current and increasing concentration of NADH. As clearly displayed in the calibration curves (inset), there is a linear relationship between the concentration of NADH and peak current as peak current increases with the increasing concentration of NADH for both di-HB-modified electrodes. Limit of detection of the electrochemical biosensor was calculated to be 4.5 μ mol $L^{-1}$ (±

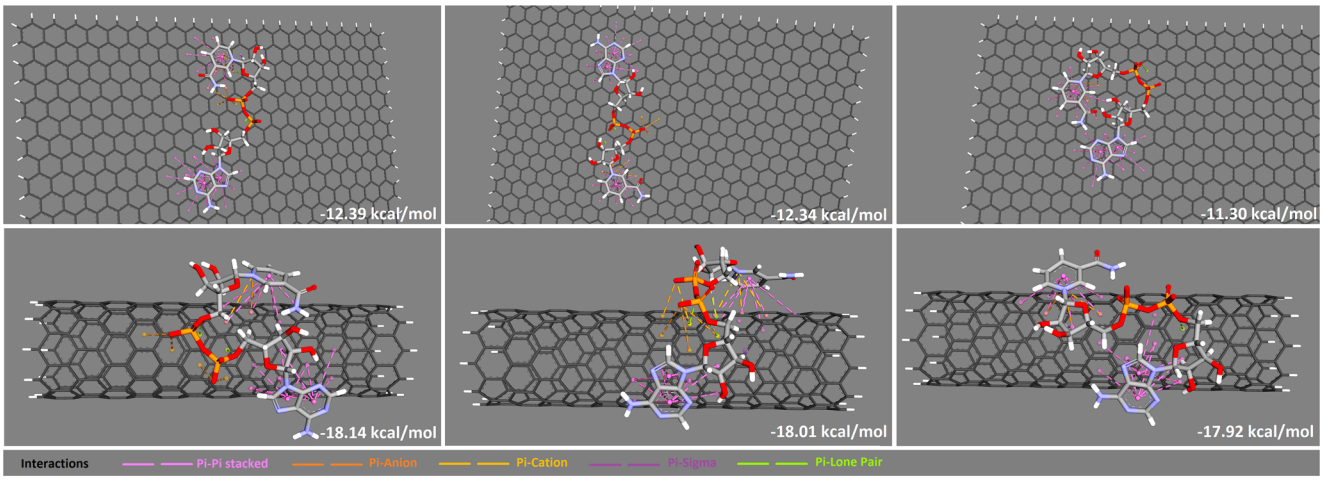


**Fig. 2** The best binding pose of $NAD^+$ for plain graphene (upper panels) and plain SWCNT (down panels)

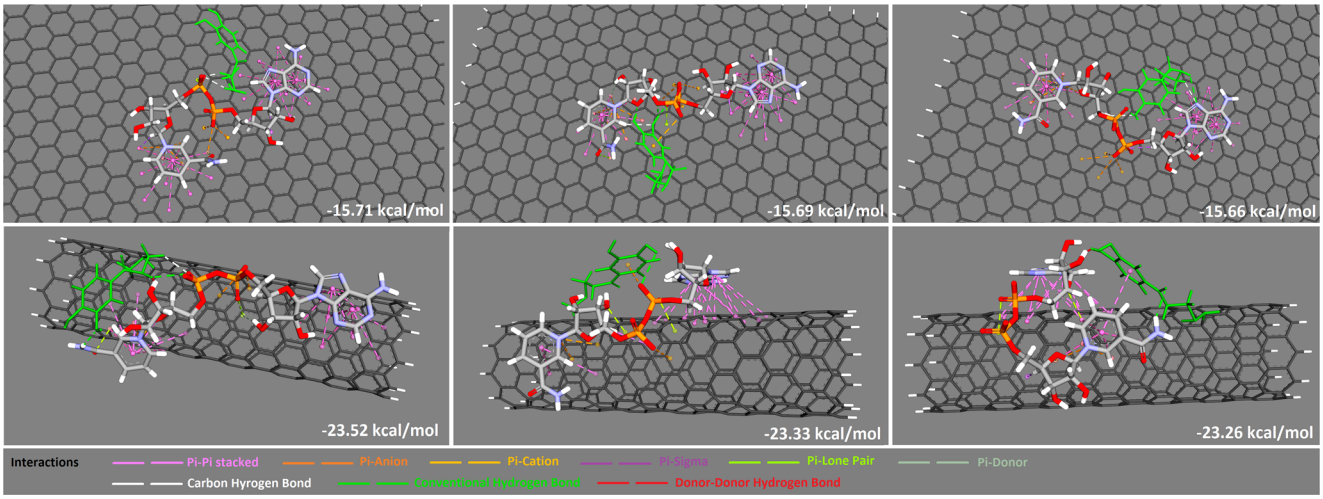


**Fig. 3** The best binding pose of $NAD^+$ for modified graphene (upper panels) and modified SWCNT (down panels) with di-HB. In here, di-HB molecule is in green

0.01) and 5.4 μ mol $L^{-1}$ (±0.07) for modified SWCNT and GO, respectively, using $3\sigma$, where $\sigma$ is standard deviation of blank solution with 6 parallel measurements.

Stability of the developed electrodes was also tested by immersing both the modified carbon electrodes into NADH solution for 1 h. CV measurement was then carried out, and very little decrease in the oxidation peak current was observed, indicating the fact that fouling of the carbon electrodes by NADH was considerably hindered. This experimental outcome might be ascribed to the fact that adsorption of NADH occurs at the edge sites of SWCNT, referring to blocking of adsorption of NADH through interaction between either di-HB or edge sites and NADH. On the basis of these findings, it could be concluded that functionalized SWCNT and GO electrodes by di-HB can be recognized as promising biosensors for practical determination of NADH.

We showed by electrochemistry that NADH oxidation at the bare SWCNT occurs more easily in comparison with unmodified GO. It was also proven that the decrease in the overpotential belonging to NADH oxidation for the di-HB-modified SWCNT is larger than GO. However, we still do not have any clue regarding the interaction mechanism at atomic level between $NAD^+$ and unmodified and di-HB-modified SWCNT and GO and reason of catalytic activity and decrease in the overpotential of NADH oxidation at the modified SWCNT and GO surfaces with dihydroxybenzene derivative. In order to investigate reaction mechanism and shed light on reason of the above-mentioned experimental findings, we have employed molecular docking simulation technique, which is a theoretical method used to support experimental results and to elucidate between substrate and receptor interactions at the molecular level. For this purpose, we performed molecular docking simulation for $NAD^+$/graphene, $NAD^+$/SWCNT, $NAD^+$/graphene/di-HB, and $NAD^+$/SWCNT/di-HB complexes. Conformations of these complexes were ranked according to calculated binding energy values, and three conformations of each complex having the highest binding energy value are listed in Table 1. As can be seen in the

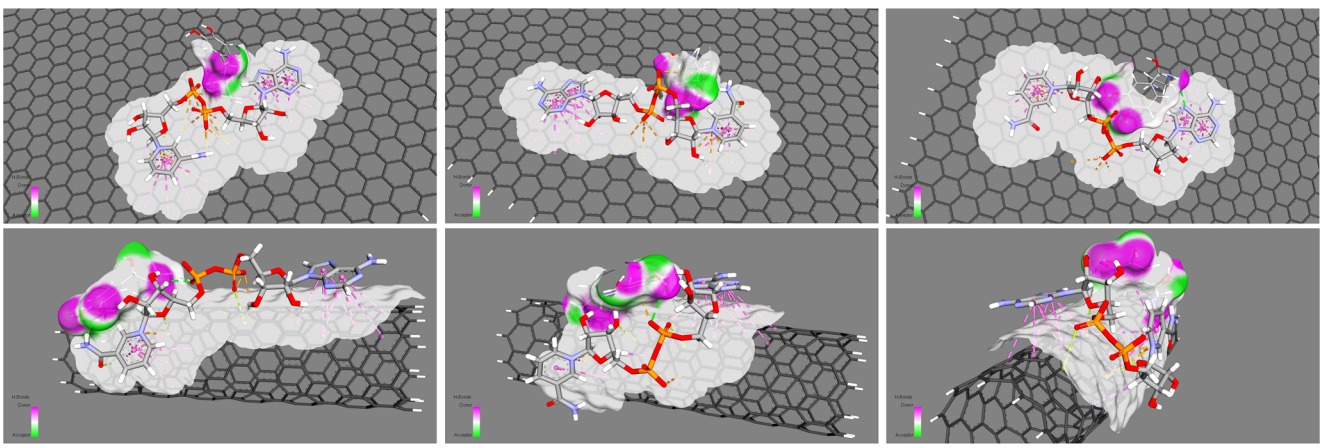

**Fig. 4** The hydrogen bond surfaces for modified graphene (upper panels) and modified SWCNT (down panels) with di-HB

**Table 2** Interaction types between $NAD^+$ and di-HB at modified target structures, number of interaction for each, and interacting atoms of $NAD^+$ and di-HB

| Target | Pose | Interactions |
|---|---|---|
| SWCNT/DHB | 1 | 1[CaH] *(14)*–**(30),** 1[CoH] *(11)*–**(30),** 1[ddH] *(11)*–**(45),** 1[CoH] *(7)*–**(6)** |
| | 2 | 1[CoH] *(22)*-**(35),** 1[pa] *(A)*-**(35)** |
| | 3 | 1[ddH] *(22)*-**(64),** 1[pp] *(A)*-**(A)**, 1[CoH] *(9)*-**(6)** |
| Graphene/DHB | 1 | 1[CaH] *(14)*-**(30),** 1[CaH] *(16)*-**(30)** |
| | 2 | 1[CaH] *(23)*-**(26),** 1[CaH] *(23)*-**(30)**, 1[CaH] *(22)*-**(20)**, 1[CoH] *(7)*-**(15)**, 1[pa] (A)-**(31)** |
| | 3 | 1[CaH] *(21)*-**(29)**, 1[CaH] *(14)*-**(51)**, 1[CoH] *(11)*-**(51),** 1[CoH] *(22)*-**(30)** |

[CaH] carbon H-bond, [CoH] conventional H-bond, [ddH] donor-donor H-bond, [pp] pi-pi stacked, [pa] pi-anion interaction. In here, atoms of $NAD^+$ is in bold text and atoms of di-HB is italic text

table, $NAD^+$ shows higher binding affinity to SWCNT surfaces (− 18.14, − 18.01, and − 17.92 kcal/mol) than graphene surfaces (− 12.39, − 12.34, and − 11.30 kcal/mol). In addition, we have observed that modification of these surfaces with di-HB significantly increases binding affinities of $NAD^+$. All these theoretical results obtained from docking simulations show good correlation with our experimental observations.

Also, three best binding poses of these complexes were visualized in Fig. 2 (plain surfaces) and Fig. 3 (modified surfaces). All interactions between $NAD^+$ and bare and modified target structures are also clearly illustrated in both figures. Besides, we have listed interaction types, the number of interaction types, and interacting atom or atom groups in detail in Table 1. The indexing of $NAD^+$ and di-HB atoms and atom groups reported in Table 1 is also displayed in Figs. S3 and S4. When table and figures are evaluated together, it is observed that the most dominant interactions between $NAD^+$ and unmodified target structures are pi-pi stacked type, which is established between the phenol and benzene rings of $NAD^+$ and the benzene rings of SWCNT or graphene surfaces. In addition, pi-anion and pi-cation-type interactions between charged groups of $NAD^+$ and graphene or SWCNT surfaces could also be considered one of the dominant interaction types here. Other interaction types and their numbers are also given detailed in Table 1.

Up to now, we have observed both theoretically and experimentally that the modification of SWCNT or graphene surfaces with di-HB enhances binding affinity of $NAD^+$. We consider that this favorable contribution to the binding energy of $NAD^+$ is mainly due to the hydrogen bond interactions formed between di-HB and $NAD^+$. We have thus plotted the hydrogen bond interaction surface areas (Fig. 4) in order to more clearly observe the characteristic behavior of main interaction type between $NAD^+$ and di-HB. The acceptor and donor surface regions of di-HB is clearly seen from Fig. 4. Also, it is seen in the surface that there is no hydrogen bond interaction between $NAD^+$ and SWCNT or graphene surfaces. In addition, all interaction types between $NAD^+$ and di-HB at the modified surfaces are given in detail in Table 2.

As a result, we have inferred that pi-type interaction between $NAD^+$ and plain graphene or SWCNT surfaces is dominant; on the other hand, the main interaction type that increased binding affinity of $NAD^+$ to the modified surfaces is due to hydrogen bonds.

## Conclusions

The functionalization of SWCNT and GO was achieved by electrochemical oxidation of Boc-protected ethylenediamine linker. Upon the deprotection of the protecting group, the coupling of di-HB that is expected to catalyze NADH oxidation to amine-terminated surface is successfully carried out by using solid-phase synthesis methodology. The electrochemical characterization of both modified surface was fulfilled by cyclic voltammetry technique. Electrochemical oxidation of NADH was investigated in both unmodified and di-HB-modified SWCNT and GO immobilized onto GC electrode. The modified SWCNT and GO electrode surfaces with di-HB were shown to possess a very good catalytic influence due to both a positive shift in peak potential of NADH oxidation and an increase in peak current with respect to both plain electrodes. We also have verified these experimental results via the molecular docking simulation method since more binding affinity energy was obtained in the case of orientation of $NAD^+$ to di-HB-modified SWCNT and GO in comparison with both unmodified surfaces due to probable formation of hydrogen bonding between NAD+ and di-HB, which was revealed through plotting the hydrogen bond interaction surface areas.

**Acknowledgments** The authors thank Zonguldak Bülent Ecevit University Faculty of Pharmacy and Science and Art for allowing to use facilities of faculties.

**Funding information** This study received financial support from Zonguldak Bülent Ecevit University Faculty of Pharmacy and Science and Art.

## References


1. Gorton L (1986) Chemically modified electrodes for the electrocatalytic oxidation of nicotinamide coenzymes. J Chem Soc, Faraday Trans 1: Phys Chem Condens Phases 82:1245–1258. https://doi.org/10.1039/F19868201245
2. Gorton L, Domınguez E (2002) Electrocatalytic oxidation of NAD(P)H at mediator-modified electrodes. Rev Mol Biotechnol 82:371–392. https://doi.org/10.1016/S1389-0352(01)00053-8
3. Bartlett PN (2008) Bioelectrochemistry: fundamentals, experimental techniques and applications. John Wiley & Sons, Chichester
4. Banks CE, Compton RG (2005) Exploring the electrocatalytic sites of carbon nanotubes for NADH detection: an edge plane pyrolytic graphite electrode study. Analyst 130:1232–1239. https://doi.org/10.1039/B508702C
5. Gao F, Yan Y, Su L, Wang L, Mao L (2007) An enzymatic glucose/O2 biofuel cell: preparation, characterization and performance in serum. Electrochem Commun 9:989–996. https://doi.org/10.1016/j.elecom.2006.12.008
6. Pérez B, del Valle M, Alegret S, Merkoçi A (2007) Carbon nanofiber vs. carbon microparticles as modifiers of glassy carbon and gold electrodes applied in electrochemical sensing of NADH. Talanta 74:398–404. https://doi.org/10.1016/j.talanta.2007.10.022
7. Pumera M (2009) The electrochemistry of carbon nanotubes: fundamentals and applications. Chem Eur J 15:4970–4978. https://doi.org/10.1002/chem.200900421
8. Pumera M, Scipioni R, Iwai H, Ohno T, Miyahara Y, Boero M (2009) A mechanism of adsorption of β-nicotinamide adenine dinucleotide on graphene sheets: experiment and theory. Chem Eur J 15:10851–10856. https://doi.org/10.1002/chem.200900399
9. Ghanem MA, Chrétien J-M, Kilburn JD, Bartlett PN (2009) Electrochemical and solid-phase synthetic modification of glassy carbon electrodes with dihydroxybenzene compounds and the electrocatalytic oxidation of NADH. Bioelectrochem 76:115–125. https://doi.org/10.1016/j.bioelechem.2009.02.008
10. Maleki A, Nematollahi D, Clausmeyer J, Henig J, Plumeré N, Schuhmann W (2012) Electrodeposition of catechol on glassy carbon electrode and its electrocatalytic activity toward NADH oxidation. Electroanal 24:1932–1936. https://doi.org/10.1002/elan.201200251
11. Matsue T, Suda M, Uchida I, Kato T, Akiba U, Osa T (1987) Electrocatalytic oxidation of NADH by ferrocene derivatives and the influence of cyclodextrin complexation. J Electroanal Chem Interfacial Electrochem 234:163–173. https://doi.org/10.1016/0022-0728(87)80169-9
12. Pinczewska A, Sosna M, Bloodworth S, Kilburn JD, Bartlett PN (2012) High-throughput synthesis and electrochemical screening of a library of modified electrodes for NADH oxidation. J Am Chem Soc 134:18022–18033. https://doi.org/10.1021/ja307390x
13. Scipioni R, Pumera M, Boero M, Miyahara Y, Ohno T (2010) Investigation of the mechanism of adsorption of β-nicotinamide adenine dinucleotide on single-walled carbon nanotubes. J Phys Chem Lett 1:122–125. https://doi.org/10.1021/jz9000714
14. Chrétien J-M, Ghanem MA, Bartlett PN, Kilburn JD (2008) Covalent tethering of organic functionality to the surface of glassy carbon electrodes by using electrochemical and solid-phase synthesis methodologies. Chem Eur J 14:2548–2556. https://doi.org/10.1002/chem.200701559
15. Ghanem MA, Chrétien J-M, Pinczewska A, Kilburn JD, Bartlett PN (2008) Covalent modification of glassy carbon surface with organic redox probes through diamine linkers using electrochemical and solid-phase synthesis methodologies. J Mater Chem 18:4917–4927. https://doi.org/10.1039/B809040H
16. Ghanem MA, Kocak I, Al-Mayouf A, AlHoshan M, Bartlett PN (2012) Covalent modification of carbon nanotubes with anthraquinone by electrochemical grafting and solid phase synthesis. Electrochim Acta 68:74–80. https://doi.org/10.1016/j.electacta.2012.02.027
17. Ghanem MA, Kocak I, Al-Mayouf A, Bartlett PN (2013) Solid phase modification of carbon nanotubes with anthraquinone and nitrobenzene functional groups. Electrochem Commun 34:258–262. https://doi.org/10.1016/j.elecom.2013.05.039
18. Manikandan A, Sathiyabama M (2015) Green synthesis of copper-chitosan nanoparticles and study of its antibacterial activity. J Nanomed Nanotech 6:1–4. https://doi.org/10.4172/2157-7439.1000251
19. Shahriary L, Athawale A (2014) Graphene oxide synthesized by using modified hummers approach. Int J Renew Energy Environ Eng 2:58–63
20. Hanwell MD, Curtis DE, Lonie DC, Vandermeersch T, Zurek E, Hutchison GR (2012) Avogadro: an advanced semantic chemical editor, visualization, and analysis platform. J Cheminformatics 4:17. https://doi.org/10.1186/1758-2946-4-17
21. Delano WL (2002) The PyMOL Molecular Graphics System. http://www.pymol.org
22. Morris GM, Huey R, Lindstrom W, Sanner MF, Belew RK, Goodsell DS, Olson AJ (2009) AutoDock4 and AutoDockTools4: automated docking with selective receptor flexibility. J Comput Chem 30:2785–2791. https://doi.org/10.1002/jcc.21256
23. Solis FJ, Wets RJ-B (1981) Minimization by random search techniques. J Math Oper Res 6:19–30. https://doi.org/10.1287/moor.6.1.19
24. Biovia DS (2017) Discovery studio modeling environment. Dassault Systèmes, San Diego
25. Chrétien J-M, Ghanem MA, Bartlett PN, Kilburn JD (2009) Covalent modification of glassy carbon surfaces by using electrochemical and solid-phase synthetic methodologies: application to bi- and trifunctionalisation with different redox centres. Chem Eur J 15:11928–11936. https://doi.org/10.1002/chem.200901135
26. Baez DF, Tapia F, Sierra-Rosales P, Bollo S (2018) In situ electroreduction of graphene oxide: increased sensitivity for the determination of NADH. Electroanalysis 30:1–8. https://doi.org/10.1002/elan.201800629